Journal of Applied and Computational Mechanics, Vol. 2, No. 4, (2016), 230-242

Shahid Chamran University

Journal of
Applied and Computational Mechanics

Uniaxial buckling analysis comparison of nanoplate and nanocomposite plate with central square cut out using domain decomposition method

Majid Jamali[1,*], Taghi Shojaee[2], Bijan Mohammadi[4]

[1]School of Mechanical Engineering, Iran University of Science and Technology, Tehran, Iran, eng.mjamali@gmail.com
[2]School of Mechanical Engineering, Iran University of Science and Technology, Tehran, Iran, ta_shojaee@cmps2.iust.ac.ir
[3]Faculty of Mechanical Engineering, University of Kashan, Kashan, Iran, r.kolahchi@gmail.com
[4]School of Mechanical Engineering, Iran University of Science and Technology, Tehran, Iran, bijan_mohammadi@iust.ac.ir

Received November 11 2016; revised December 2 2016; accepted December 23 2016
Corresponding author: Majid Jamali, eng.mjamali@gmail.com

Abstract

A comparison of buckling analysis of the nanoplate and nanocomposite plate with central square hole embedded in Winkler foundation is presented in this article. In order to enhance mechanical properties of nanoplate with central cut out, carbon nano tubes (CNTs) are applied as uniform distribution (UD) through thickness direction. In order to define the shape function of plate with square cut out, domain decomposition method and orthogonal polynomials are used. At last, to obtain critical buckling load of system, Rayleigh-Ritz energy method is provided. The impacts of the length and width of plate, dimension of square cut out and elastic medium on nanoplate and nanocomposite plate are presented in this study.

Keywords: Analytical buckling; Nanocomposite plate; Central square hole; Winkler foundation; Domain decomposition method; Rayleigh-Ritz energy method

1. Introduction

Nowadays, composite materials are applied as modern generation materials in industry and they are used instead of conventional material such as metallic, woody and concrete materials. Development of material science beside appearance of novel branch of science which is called nanotechnology caused a modern group of composites entitled nano composites. Nano composites are a branch of composite materials that their reinforcing factor has nano scale. Marvelous discovery and invention of CNTs with extraordinary mechanical, thermal, electric and magnetic properties tempted researchers to apply CNTs for reinforcing composites. Some significant applications of nano composites are, abrasion resistant coatings, corrosion resistant coatings, conductive plastics, sensors, resistant lining in high temperature and separation membranes for gases and petroleum fluids.

Buckling analysis of nanoplates has been considered by many researchers hitherto. Murmu and Pradhan [1] investigated the elastic buckling behavior of orthotropic small scale plates under biaxial compression. This study discussed the effects of the small scale on the buckling loads of nanoplates assuming various material and geometrical parameters. Buckling of single layer graphene sheet (SLGS) based on nonlocal elasticity and higher order shear deformation theory was addressed by Pradhan [2]. Levy type solution method for vibration and buckling of nanoplates using nonlocal elasticity theory was reported by Aksencer and Aydogdu [3]. Results presented for different nonlocal parameter, different length of plates and different boundary conditions. In addition, results demonstrated that nonlocal effects for nanoscale plates should be considered. Hashemi and Samaei [4] carried out the buckling analysis of micro/nanoscale plates via nonlocal elasticity theory. The effect of length scale on buckling behavior of a SLGS embedded in a Pasternak elastic medium using a nonlocal Mindlin plate theory was discussed by Samaei et al. [5]. It is understood that the nonlocal assumptions present larger buckling loads and stiffness of elastic medium in comparison with classical plate theory (CPT). Farajpour et al. [6] reported buckling analysis of variable thickness nanoplates using nonlocal continuum mechanics. Result showed that the influence of percentage change of thickness on the stability of graphene sheets is more remarkable in the strip-type nanoplates (nanoribbons) than in the

square-type nanoplates. Buckling response of orthotropic SLGS is investigated applying the nonlocal elasticity theory proposed by Farajpour et al. [7]. Differential quadrature method (DQM) has been applied to solve the governing equations for various boundary conditions. It is explicit that the nonlocal effects play a considerable role in the stability behavior of orthotropic nanoplates. Murmu et al. [8] addressed nonlocal buckling of double-nanoplate-systems (DNPS) under biaxial compression. Both synchronous and asynchronous buckling phenomenon of biaxially compressed DNPS is presented in this work. Buckling analysis of double-orthotropic nanoplates embedded in Pasternak elastic medium using nonlocal elasticity theory was discussed by Radić et al. [9]. The influence of small scale coefficient, aspect ratio, and stiffness of internal elastic media and external elastic foundation, on the nondimensional buckling was considered. Golmakania and Rezatalab [10] proposed the nonuniform biaxial buckling of orthotropic nanoplates embedded in an elastic medium based on nonlocal Mindlin plate theory. The effect of small scale effect, aspect ratio, polymer matrix properties, type of planar loading, mode numbers and boundary conditions were probed in details.

CNTs can be used as amplifier in different structure (beam, plate, etc.) and produce nanocomposite system in order to enhance mechanical properties and improve behavior of system. Buckling analysis of laminated composite rectangular plates reinforced by CNTs using analytical and finite element methods was carried out by Ghorbanpour Arani et al. [11].In this article, the effects of the CNTs orientation angle, the edge conditions, and the aspect ratio on the critical buckling load are considered using both the analytical and finite element methods. The critical buckling load of composite rectangle plate reinforced with CNTs subjected to axial compressive load using CPT is discussed by Jam and Maghamikia [12]. Mohammadimehr et al. [13] proposed the buckling and vibration analysis of a double-bonded nanocomposite piezoelectric plate reinforced by boron nitride nanotube based on the Eshelby-Mori-Tanaka approach applying modified couple stress theory under electro-thermo-mechanical loadings surrounded by an elastic foundation. The buckling analysis of annular composite plates reinforced by CNTs subjected to compressive and torsional loads was addressed by Asadi and Jam [14]. It is concluded that the stability of plate increases as the thickness or inner to outer ratio rises and when the CNTs arranged in the circumferential direction the highest buckling load is obtained. Mohammadimehr et al. [15] analyzed the biaxial buckling and bending of smart nanocomposite plate reinforced by CNTs using extended mixture rule approach.

Considering the literature, no report has studied the buckling analysis of nano plate with square cut out. These considerations stimulated us to present buckling analytical investigation of nano plate and nanocomposite plate with square cut out embedded by Winkler medium. CPT is applied to simulate plate and rule of mixture is used to obtain the mechanical properties of nanocomposite plate. A detailed parametric study is conducted to explicit the effects of the dimensions of plate, length of square cut out and elastic medium on buckling analysis.

2. Nanocomposite Plate

Consider a nanocomposite plate as illustrated in Fig. 1, with the length of *a*, width *b* and thickness *h* and a central square hole with length *d*. The plate is subjected to uniaxial load along x-direction (N_x) and surrounded by Winkler foundation. Moreover, the plate is reinforced by CNTs through thickness direction.

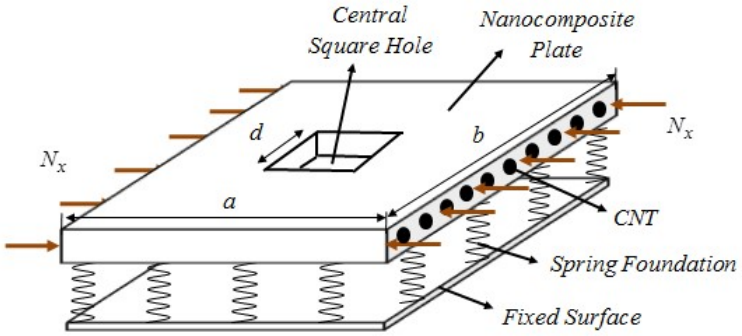

Fig. 1. A nanocomposite cut out plate subjected to uniaxial buckling load surrounded by Winkler foundation.

The plate is assumed to be isotropic but after using orthotropic CNTs in it, the system change to orthotropic structure. Therefore, by using CNTs in plate mechanical properties of system will be improved, thus, the effective mechanical properties of nanocomposite plate are extended through the rule of mixture and Young's modulus, E_{11} and E_{22}, and shear modulus, G_{12}, are [16, 17]

$$E_{11} = \eta_1 V_{CNT} E_{11}^{CNT} + V_m E^m, \tag{1}$$

$$\frac{\eta_2}{E_{22}} = \frac{V_{CNT}}{E_{22}^{CNT}} + \frac{V_m}{E^m}, \tag{2}$$

$$\frac{\eta_3}{G_{12}}=\frac{V_{CNT}}{G_{12}^{CNT}}+\frac{V_m}{G^m}, \tag{3}$$

in which E_{11}^{CNT}, E_{22}^{CNT} and G_{12}^{CNT} are Young's modulus and shear modulus of CNTs, respectively and E^m, G^m show the corresponding properties related to matrix. The CNT efficiency parameters, $\eta_j\ (j=1,2,3)$, demonstrate the scale-dependent material properties obtained by matching the effective mechanical properties of nanocomposite plate calculated from the MD simulations with those from the rule of mixture. The relation between volume fractions of CNT, V_{CNT}, and volume fractions of matrix, V_m, expressed as

$$V_{CNT}+V_m=1. \tag{4}$$

where for UD type

$$V_{CNT}=\frac{W_{CNT}}{W_{CNT}+\left(\frac{\rho_{CNT}}{\rho_m}\right)-\left(\frac{\rho_{CNT}}{\rho_m}\right)W_{CNT}}, \tag{5}$$

in which w_{CNT} expresses the mass fraction of nanotube. The Poisson's ratio, υ_{12}, of the nanocomposite plate is

$$\upsilon_{12}=V_{CNT}\upsilon_{12}^{CNT}+V_m\upsilon^m, \tag{6}$$

where υ_{12}^{CNT} and υ^m are Poisson's ratios of CNTs and plate, respectively.

The constitutive equations of the nonlocal elasticity are

$$\begin{Bmatrix}\sigma_{xx}\\ \sigma_{yy}\\ \sigma_{xy}\end{Bmatrix}=\begin{pmatrix}C_{11} & C_{12} & 0\\ C_{12} & C_{22} & 0\\ 0 & 0 & C_{66}\end{pmatrix}\begin{Bmatrix}\varepsilon_{xx}\\ \varepsilon_{yy}\\ \varepsilon_{xy}\end{Bmatrix}, \tag{7}$$

in which σ_{ij} and ε_{ij} are stress and strain, respectively. C_{ij} are elasticity coefficients and with respect to orthotropic structure, they are considered as [18]

$$C_{11}=\frac{E_{11}}{1-\upsilon_{12}\upsilon_{21}},C_{22}=\frac{E_{22}}{1-\upsilon_{12}\upsilon_{21}},C_{12}=\frac{\upsilon_{21}E_{11}}{1-\upsilon_{12}\upsilon_{21}},C_{66}=G_{12}. \tag{8}$$

3. Plate Theory

The CPT is derived from Euler–Bernoulli beam theory for thin plates. This theory is based on following assumptions as

- After displacement, straight lines normal to the mid-surface stay straight.
- After displacement, straight lines normal to the mid-surface stay normal.
- During displacement, thickness of the plate remains and does not change.

According to the CPT, the displacement field can be considered as [19, 20]

$$u(x,y,z)=z\beta_x, \tag{9}$$

$$v(x,y,z)=z\beta_y, \tag{10}$$

$$w=w(x,y), \tag{11}$$

where, *u*, *v* and *w* denote the displacement vector along x- , y- and z-direction , respectively.

β_x and β_y are rotation around x- and y-direction expressed as

$$\beta_x=-\frac{\partial w}{\partial x}, \tag{12}$$

$$\beta_y=-\frac{\partial w}{\partial y}, \tag{13}$$

The von Karman strains based on above displacement field can be calculated as

$$\varepsilon_x=-z\frac{\partial^2}{\partial x^2}w(x,y), \tag{14}$$

$$\varepsilon_y = -z\frac{\partial^2}{\partial y^2}w(x,y), \tag{15}$$

$$\gamma_{xy} = -2z\frac{\partial^2}{\partial x\,\partial y}w(x,y), \tag{16}$$

where ε_x , ε_y and γ_{xy} are the normal strain along x and y axis and the shear strain component, respectively.

4. Nonlocal Elasticity Theory and Energy Method

In nano/micro scale local theory is not valid and some other theories are suggested such as Eringen's nonlocal elasticity theory. This theory expresses that the stress state at a reference point in the body is not related only to the strain state at this point but also on the strain states at all of the points throughout the body. According to this theory it can be express as [21]

$$\left(1-\mu^2\nabla^2\right)\sigma_{ij}^{nl} = \sigma_{ij}^{l}, \tag{17}$$

where the parameter $\mu = (e_0 a)^2$ demonstrates the small scale effect regard to nanoscale, and ∇^2 is the Laplacian operator. It should be represented that the nonlocal stresses tensor change to a local one when the nonlocal parameter set to zero.

Energy method is applied to obtain equations of system as [22]

$$\Pi = U - W, \tag{18}$$

where, U and W are strain energy and external works, respectively and Π is total energy of system.

4.1. Strain energy

Strain energy can be obtained as [23]

$$U = \frac{1}{2}\int_A\int_{\frac{-h}{2}}^{\frac{h}{2}}\left(\sigma_{xx}\varepsilon_{xx} + \sigma_{yy}\varepsilon_{yy} + \sigma_{xy}\gamma_{xy}\right)dz\,dA. \tag{19}$$

By substituting Eqs.(14-16) and Eq.(7) into Eq.(19)

$$U = \frac{1}{2}\int_A\left(-M_x\frac{\partial^2}{\partial x^2}w(x,y) - 2M_{xy}\frac{\partial^2}{\partial y\,\partial x}w(x,y) - M_y\frac{\partial^2}{\partial y^2}w(x,y)\right)dA \tag{20}$$

in which moment resultants are considered as [24]

$$\left(M_x, M_y, M_{xy}\right) = \int_{\frac{-h}{2}}^{\frac{h}{2}}(\sigma_x, \sigma_y, \sigma_{xy})\,z\,dz, \tag{21}$$

4.2. External works

According to Fig. 1, the nanocomposite plate is subjected to two types of forces such as:

4.2.1. Foundation forces

The plate is embedded by Winkler foundation; as it is known, this foundation model considers normal load from environment to system. Therefore, the work of this foundation can be obtained as [25]

$$W_e = -\int_A\left(K_w w\right)w\,dA, \tag{22}$$

K_w is Winkler's spring modulus.

4.2.2. Buckling load

The nanocomposite plate is subjected to buckling, thus the work of this force can be calculated as [22]

$$W_b = -\frac{1}{2}\int_A\left(N_{xx}\left(\frac{\partial}{\partial x}w(x,y)\right)^2 + N_{yy}\left(\frac{\partial}{\partial y}w(x,y)\right)^2\right)dA, \tag{23}$$

the buckling load is uniaxial, so $N_{xx} = -P$ and $N_{yy} = 0$.

With respect to Eringen's nonlocal elasticity theory and energy method, total energy of nanocomposite plate is equal to

$$\Pi = \int_A \left(\mu^2 P \left(\frac{\partial^2 w}{\partial x^2} \right)^2 + \mu^2 P \left(\frac{\partial^2 w}{\partial y \partial x} \right)^2 - \frac{1}{2} P \left(\frac{\partial w}{\partial x} \right)^2 + \mu^2 P \left(\frac{\partial w}{\partial x} \right) \left(\frac{\partial^3 w}{\partial x^3} \right) + \mu^2 P \left(\frac{\partial w}{\partial x} \right) \left(\frac{\partial^3 w}{\partial y^2 \partial x} \right) \right.$$
$$-2\mu^2 K_w w \left(\frac{\partial^2 w}{\partial x^2} \right) - 2\mu^2 K_w w \left(\frac{\partial^2 w}{\partial y^2} \right) - 2\mu^2 K_w \left(\frac{\partial w}{\partial y} \right)^2 + K_w w^2 - 2\mu^2 K_w \left(\frac{\partial w}{\partial x} \right)^2 \tag{24}$$
$$\left. -\frac{1}{2} M_x \left(\frac{\partial^2 w}{\partial x^2} \right) - M_{xy} \left(\frac{\partial^2 w}{\partial y \partial x} \right) - \frac{1}{2} M_y \left(\frac{\partial^2 w}{\partial y^2} \right) \right) dA ,$$

where

$$M_x = -D_{11} \left(\frac{\partial^2}{\partial x^2} w(x,y) \right) h - D_{12} \left(\frac{\partial^2}{\partial y^2} w(x,y) \right) h , \tag{25}$$

$$M_y = -D_{12} \left(\frac{\partial^2}{\partial x^2} w(x,y) \right) h - D_{22} \left(\frac{\partial^2}{\partial y^2} w(x,y) \right) h , \tag{26}$$

$$M_{xy} = -2 D_{66} \left(\frac{\partial^2}{\partial y \partial x} w(x,y) \right) h , \tag{27}$$

and the stiffness components in aforementioned equations can be specified as [16]

$$(D_{11}, D_{22}, D_{12}, D_{66},) = \int_{-\frac{h}{2}}^{\frac{h}{2}} z^2 . (C_{11}(z), C_{22}(z), C_{12}(z), C_{66}(z)) dz , \tag{28}$$

5. Buckling of Cut out Nanocomposite Plate

5.1. Domain decomposition method and orthogonal polynomials

In this section, the shape function of plate with central cut out in simply supported boundary conditions (S-S-S-S), will be calculated by applying domain decomposition method and orthogonal polynomials. At first domain decomposition method [22, 26-33], which considers not only the outer boundary conditions (S-S-S-S), but also the inner (cut out edges) free boundary condition, is used to divide plate to some sub-domain. Because of the two symmetrical conditions only one quarter of the rectangular plate with a central square cut out need to be considered as Fig. 2, therefore, one fourth of plate is divided to three sub-domains.

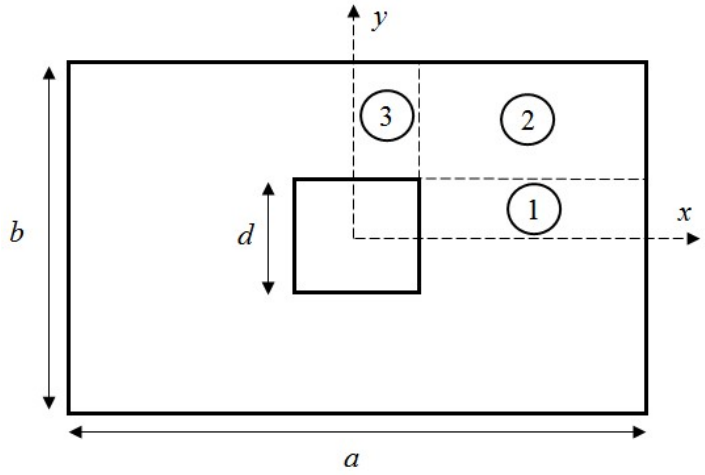

Fig. 2. Illustration of dividing the nanocomposite cut out plate to three sub-domains.

After partitioning nanocomposite plate with a central square cut out, shape function should be determined. Orthogonal polynomials [31] are applied to present the shape function of each sub-domain which considers the geometric boundary conditions. The deflection shape functions for each sub-domain can be defined as

$$w^{(1)}(x,y) = \sum_{m=1}^{M} \sum_{n=1}^{N} A_{mn}^{(1)} f_m^{(1)}(x) g_n^{(1)}(y) , \tag{29}$$

$$w^{(2)}(x,y) = \sum_{m=1}^{M} \sum_{n=1}^{N} A_{mn}^{(2)} f_m^{(2)}(x) g_n^{(2)}(y) , \tag{30}$$

$$w^{(3)}(x,y)=\sum_{m=1}^{M}\sum_{n=1}^{N}A_{mn}^{(3)}f_m^{(3)}(x)g_n^{(3)}(y), \tag{31}$$

where, the superscripts (1), (2) and (3) are imply to sub-domain 1, 2 and 3 respectively. $w^{(i)}(i=1,2,3)$ are the shape functions of sub-domain 1, 2 and 3 respectively. $A_{mn}^{(i)}$ are the undetermined coefficients of the shape functions $w^{(i)}$. $f_m^{(i)}(x)$ are polynomial functions which consider the essential boundary conditions along x-direction, while $g_n^{(i)}(y)$ are polynomial functions which consider the essential boundary conditions along y-direction. The orthogonal polynomial functions $f_m^{(i)}(x)$ and $g_n^{(i)}(y)$ are made by the Gram–Schmidt process [31], applying the initial polynomials $(f_1(x), g_0(x))$ which initially satisfy the essential boundary conditions, can be calculated for different boundary conditions according to Table 1. The process is as [31]

$$f_2(x)=(g_0(x)-A_1)f_1(x), \tag{32}$$

$$f_{k+1}(x)=(g_0(x)-A_k)f_k(x)-B_k f_{k-1}(x),\ k\geq 2 \tag{33}$$

where

$$A_k=\frac{\int_0^1 g_0(x)f_k(x)f_k(x)dx}{\int_0^1 f_k(x)f_k(x)dx}, \tag{34}$$

$$B_k=\frac{\int_0^1 g_0(x)f_k(x)f_{k-1}(x)dx}{\int_0^1 f_{k-1}(x)f_{k-1}(x)dx}. \tag{35}$$

In order to specify functions $g_n(y)$ the same process of determining $f_m(x)$ as defined in Eqs. (32-35) can be used.

Therefore, shape functions of three sub-domains were defined hitherto and the final step in order to calculate buckling load, is to determine deflection functions of three sub-domains in terms of the undetermined coefficients of one the sub-domains. Thus, the best way is to apply some spots

Table 1. Starting polynomials for sets of orthogonal polynomials [22].

Boundary Conditions	Starting Polynomials, $f_1(x)$	Generating Functions, $g_0(x)$
Free-Free $f_1''(0)=f_1'''(0)=0,$ $f_1''(1)=f_1'''(1)=0$	1.0	x
Free-Simply supported $f_1''(0)=f_1'''(0)=0,$ $f_1(1)=f_1''(1)=0$	$1-x$	x^2-2x
Free-Clamped $f_1''(0)=f_1'''(0)=0,$ $f_1(1)=f_1'(1)=0$	$3-4x+x^4$	x
Symmetric-Free $f_1'(0)=f_1'''(0)=0,$ $f_1''(1)=f_1'''(1)=0$	$1+x^2$	$1+x^2$
Symmetric- Simply supported $f_1'(0)=f_1'''(0)=0,$ $f_1(1)=f_1''(1)=0$	$5-6x^2+x^4$	x^2
Symmetric- Clamped		

$f_1'(0)=f_1'''(0)=0,$ $f_1(1)=f_1'(1)=0$	$1-2x^2+x^4$	$1-x^2$
Anti-symmetric- Simply supported		
$f_1(0)=f_1''(0)=0,$ $f_1(1)=f_1''(1)=0$	$x-2x^3+x^4$	x^2

in the interconnecting boundary between sub-domains and according to the mathematical derivation, the undetermined coefficients of sub-domains 1, 2 and 3 are related together [30-33].

5.2. Rayleigh-Ritz method

Rayleigh-Ritz method is used to calculate buckling load of nanocomposite plate with a central square cut out. As noted before, because of the two symmetrical conditions only one quarter of the rectangular plate with a central square cut out need to be considered. The total energy of cut out plate is determined as

$$\Pi = \Pi^{(1)} + \Pi^{(2)} + \Pi^{(3)}, \tag{36}$$

$\Pi^{(i)}\,(i=1,2,3)$ are total energy of sub-domains 1, 2 and 3, respectively and they are defined with respect to Eq. (24) and Fig. 2 as

$$\begin{aligned}\Pi^{(1)} = \int_0^{\frac{d}{2}}\int_{\frac{d}{2}}^{\frac{a}{2}}\Bigg(&\mu^2 P\left(\frac{\partial^2 w^{(1)}}{\partial x^2}\right)^2+\mu^2 P\left(\frac{\partial^2 w^{(1)}}{\partial y\,\partial x}\right)^2-\frac{1}{2}P\left(\frac{\partial w^{(1)}}{\partial x}\right)^2+\mu^2 P\left(\frac{\partial w^{(1)}}{\partial x}\right)\left(\frac{\partial^3 w^{(1)}}{\partial x^3}\right)+\mu^2 P\left(\frac{\partial w^{(1)}}{\partial x}\right)\left(\frac{\partial^3 w^{(1)}}{\partial y^2\,\partial x}\right)\\&-2\mu^2 K_w w^{(1)}\left(\frac{\partial^2 w^{(1)}}{\partial x^2}\right)-2\mu^2 K_w w^{(1)}\left(\frac{\partial^2 w^{(1)}}{\partial y^2}\right)-2\mu^2 K_w\left(\frac{\partial w^{(1)}}{\partial y}\right)^2+K_w\left(w^{(1)}\right)^2-2\mu^2 K_w\left(\frac{\partial w^{(1)}}{\partial x}\right)^2\\&-\frac{1}{2}M_x\left(\frac{\partial^2 w^{(1)}}{\partial x^2}\right)-M_{xy}\left(\frac{\partial^2 w^{(1)}}{\partial y\,\partial x}\right)-\frac{1}{2}M_y\left(\frac{\partial^2 w^{(1)}}{\partial y^2}\right)\Bigg)dx\,dy,\end{aligned} \tag{37}$$

$$\begin{aligned}\Pi^{(2)} = \int_{\frac{d}{2}}^{\frac{b}{2}}\int_{\frac{d}{2}}^{\frac{a}{2}}\Bigg(&\mu^2 P\left(\frac{\partial^2 w^{(2)}}{\partial x^2}\right)^2+\mu^2 P\left(\frac{\partial^2 w^{(2)}}{\partial y\,\partial x}\right)^2-\frac{1}{2}P\left(\frac{\partial w^{(2)}}{\partial x}\right)^2+\mu^2 P\left(\frac{\partial w^{(2)}}{\partial x}\right)\left(\frac{\partial^3 w^{(2)}}{\partial x^3}\right)+\mu^2 P\left(\frac{\partial w^{(2)}}{\partial x}\right)\left(\frac{\partial^3 w^{(2)}}{\partial y^2\,\partial x}\right)\\&-2\mu^2 K_w w^{(2)}\left(\frac{\partial^2 w^{(2)}}{\partial x^2}\right)-2\mu^2 K_w w^{(2)}\left(\frac{\partial^2 w^{(2)}}{\partial y^2}\right)-2\mu^2 K_w\left(\frac{\partial w^{(2)}}{\partial y}\right)^2+K_w\left(w^{(2)}\right)^2-2\mu^2 K_w\left(\frac{\partial w^{(2)}}{\partial x}\right)^2\\&-\frac{1}{2}M_x\left(\frac{\partial^2 w^{(2)}}{\partial x^2}\right)-M_{xy}\left(\frac{\partial^2 w^{(2)}}{\partial y\,\partial x}\right)-\frac{1}{2}M_y\left(\frac{\partial^2 w^{(2)}}{\partial y^2}\right)\Bigg)dx\,dy,\end{aligned} \tag{38}$$

$$\begin{aligned}\Pi^{(3)} = \int_{\frac{d}{2}}^{\frac{b}{2}}\int_0^{\frac{d}{2}}\Bigg(&\mu^2 P\left(\frac{\partial^2 w^{(3)}}{\partial x^2}\right)^2+\mu^2 P\left(\frac{\partial^2 w^{(3)}}{\partial y\,\partial x}\right)^2-\frac{1}{2}P\left(\frac{\partial w^{(3)}}{\partial x}\right)^2+\mu^2 P\left(\frac{\partial w^{(3)}}{\partial x}\right)\left(\frac{\partial^3 w^{(3)}}{\partial x^3}\right)+\mu^2 P\left(\frac{\partial w^{(3)}}{\partial x}\right)\left(\frac{\partial^3 w^{(3)}}{\partial y^2\,\partial x}\right)\\&-2\mu^2 K_w w^{(3)}\left(\frac{\partial^2 w^{(3)}}{\partial x^2}\right)-2\mu^2 K_w w^{(3)}\left(\frac{\partial^2 w^{(3)}}{\partial y^2}\right)-2\mu^2 K_w\left(\frac{\partial w^{(3)}}{\partial y}\right)^2+K_w\left(w^{(3)}\right)^2-2\mu^2 K_w\left(\frac{\partial w^{(3)}}{\partial x}\right)^2\\&-\frac{1}{2}M_x\left(\frac{\partial^2 w^{(3)}}{\partial x^2}\right)-M_{xy}\left(\frac{\partial^2 w^{(3)}}{\partial y\,\partial x}\right)-\frac{1}{2}M_y\left(\frac{\partial^2 w^{(3)}}{\partial y^2}\right)\Bigg)dx\,dy,\end{aligned} \tag{39}$$

Therefore, total energy of cut out plate is specified in terms of the undetermined coefficients of shape function of sub-domain 1. The critical buckling load of the cut out plate after applying Rayleigh-Ritz method is determined by putting the coefficient determinant of the equations equal to zero.

6. Results

The results of buckling analysis associated with nano plate and nanocomposite plate with centeral square cut out surrounded by winkler foundation are provided in this sector. The goal of this essay is to consider the effects of the dimensions of plate, length of square cut out and elastic medium on critical buckling load of plate. Here Poly-co-vinylene, referred to as PmPV, and orthotropic CNTs are selected as the matrix and the reinforcement materials, respectively. The material properties of CNTs and PmPV are addressed in Table 2 [34].

Table 2. Material properties of matrix and CNTs [34].

Matrix	CNTs
$E^m = 2.1(GPa)$	$E_{11}^{CNT} = 5.6466(TPa)$
$\upsilon_m = 0.34$	$E_{22}^{CNT} = 7.08(TPa)$
	$G_{12}^{CNT} = 1.9447(TPa)$
	$\upsilon_{12}^{CNT} = 0.175$

Table 3 provides buckling load for different values of nonlocal parameter and aspect ratio of length to thickness. As can be seen, the present results match closely with those defined by Hashemi and Samaei [4], Pradhan and Murmu [35] and Pradhan [2].

In this editorial, buckling load ratio and dimensionless Winkler modulus are determined as ($Buckling\ load\ ratio = \frac{Buckling\ load\ from\ nonlocal\ theory\ (P_{nl})}{Buckling\ load\ from\ local\ theory\ (P_l)}$) and ($K_W = \frac{K_w\ h}{E^m}$), respectively.

Fig. 3 shows the effect of CNTs in plate on buckling load ratio with respect to nonlocal parameter. It is distinct that Isotropic type (plate without CNTs) has minimum effect on critical buckling load ratio in comparison with Composite type which CNTs are as amplifier in plate. However, it can be comprehend that CNTs can enhance the mechanical properties of plate and then critical buckling load ratio increases.

Table 3. A comparison between the buckling analysis of SLGS using the theories of classical plate, higher order shear deformation and Mindlin plate.

a/h	e_0a	CPT [35]	higher order plate theory [2]	Mindlin plate theory [4]	present
100	0.0	9.8791	9.8671	9.8671	9.8790
	0.5	9.4156	9.4031	9.4029	9.4156
	1.0	8.9947	8.9807	8.9803	8.9945
	1.5	8.6073	8.5947	8.5939	8.6073
	2.	8.2537	8.2405	8.2393	8.2533
20	0.0	9.8177	9.8067	9.8067	9.8172
	0.5	9.3570	9.3455	9.3455	9.3570
	1.0	8.9652	8.9528	8.9527	8.9648
	1.5	8.5546	8.5420	8.5420	8.5546
	2.0	8.2114	8.1900	8.1898	8.2111

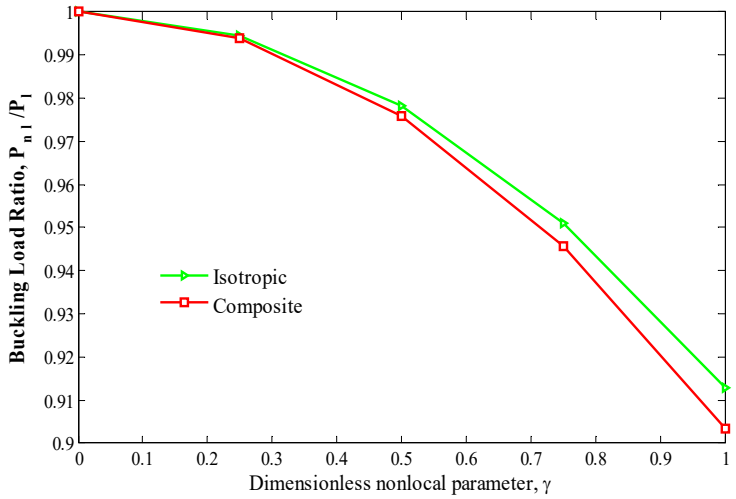

Fig. 3. A comparison between Isotropic and Composite types on buckling load ratio versus dimensionless nonlocal parameter.

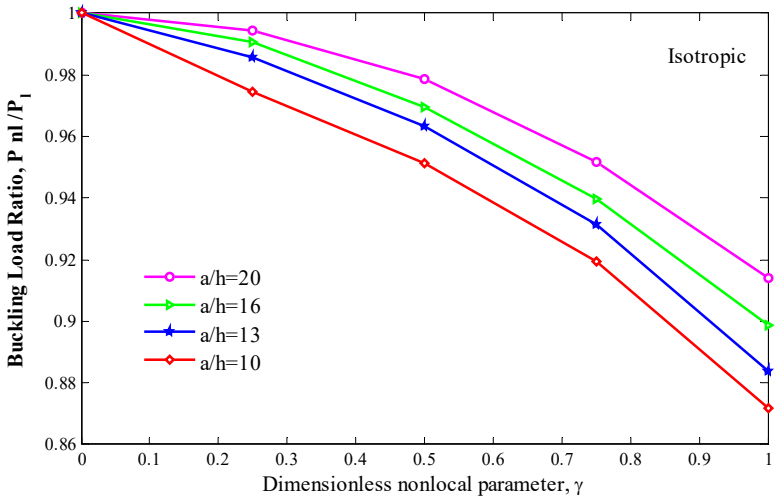

Fig. 4a

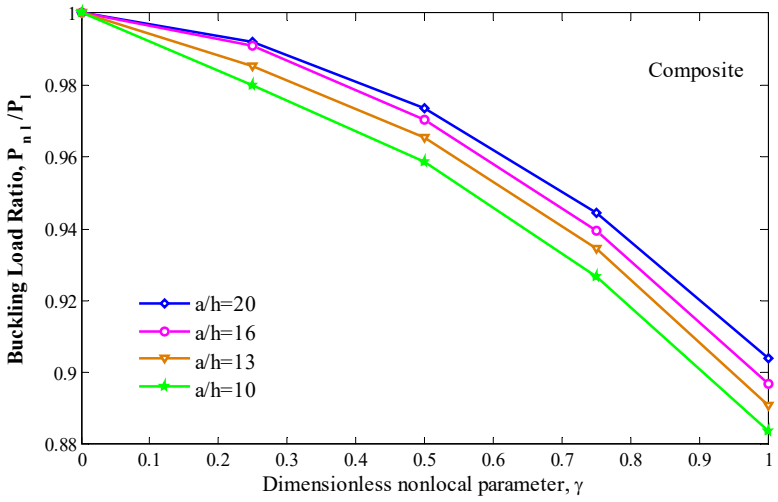

Fig. 4b

Fig. 4. Effect of the length of plate on critical buckling load ratio in terms of the dimensionless nonlocal parameter.

Fig. 4 illustrates the effect of length of plate on buckling load ratio by considering dimensionless nonlocal parameter. As can be seen, by increasing nonlocal parameter, critical buckling load ratio decreases. The figure shows that increase length causes more buckling load ratio, because by increasing length, stiffness of system decreases so the critical buckling load decreases too but variation of local buckling load is more than nonlocal buckling load, therefore, the critical buckling load ratio increases. It is apparent that the effect of length on the buckling load ratio is more remarkable in high value of nonlocal parameter.

Variation of critical buckling load ratio in terms of nonlocal parameter with respect to different aspect ratio of nanocomposite square cut out plate is analyzed in Fig. 5. It is obvious that the effectiveness order of aspect ratio on buckling load ratio from high to low is as $a/b\rangle 1$, $a/b=1$ and $a/b\langle 1$, respectively. To understand the reason of this order, it is better to look at Fig. 1 and consider the length and width of plate and the direction of uniaxial buckling load. Moreover, by keep in view to the trend of figure, buckling load ratio decreases by increasing nonlocal parameter.

Now the effect of the elastic medium on critical buckling ratio is examined in this section. Fig. 7 analyzes the variation of buckling load ratio by considering nonlocal parameter keep in view different magnitude of Winkler modulus parameter (K_W). It is obvious that considering Winkler modulus parameter improves the buckling behavior of plate, because Winkler foundation imposes normal force to system, therefore, considering these foundation increase the stiffness of system and buckling load ratio.

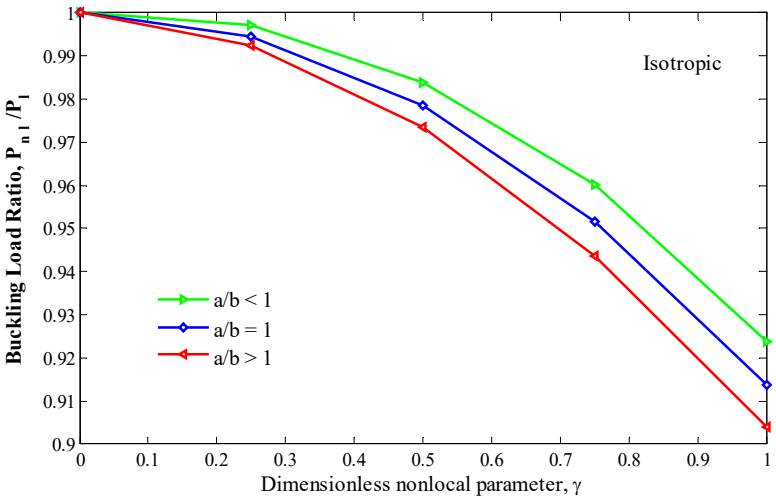

Fig. 5a

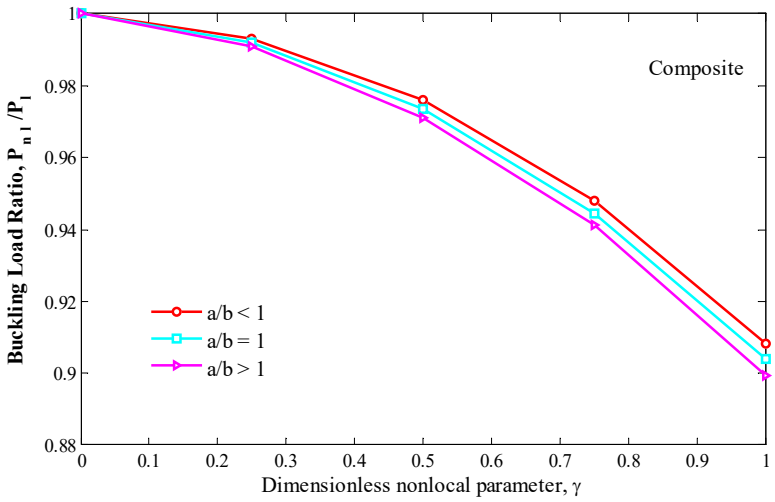

Fig. 5a

Fig. 5. Effect of the aspect ratio of plate on buckling load ratio versus the dimensionless nonlocal parameter.

Fig. 6 considers the effect of length of square cut out in nanocomposite plate on buckling load ratio in terms of the nonlocal parameter. It is apparent, existence a hole in plate causes defect in system and weaken the buckling behavior, therefore, by increasing length of square cut out in plate buckling load ratio increase. In addition, the effect of length of hole on critical buckling load ratio is more considerable for high dimensionless nonlocal parameter.

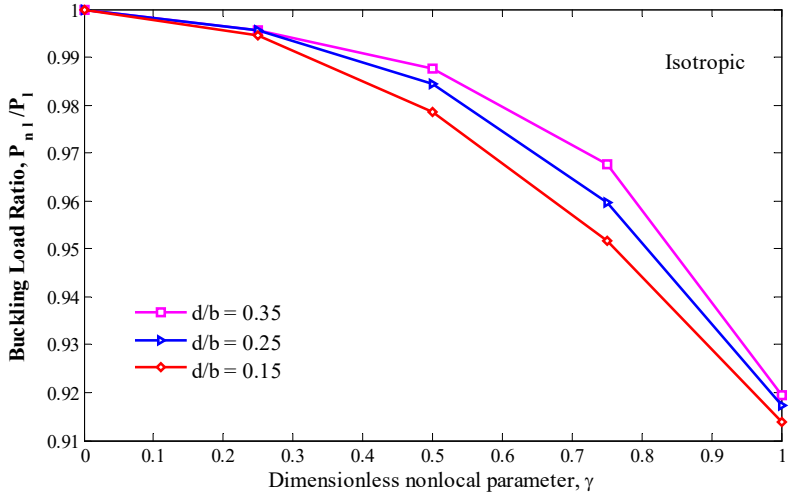

Fig. 6a

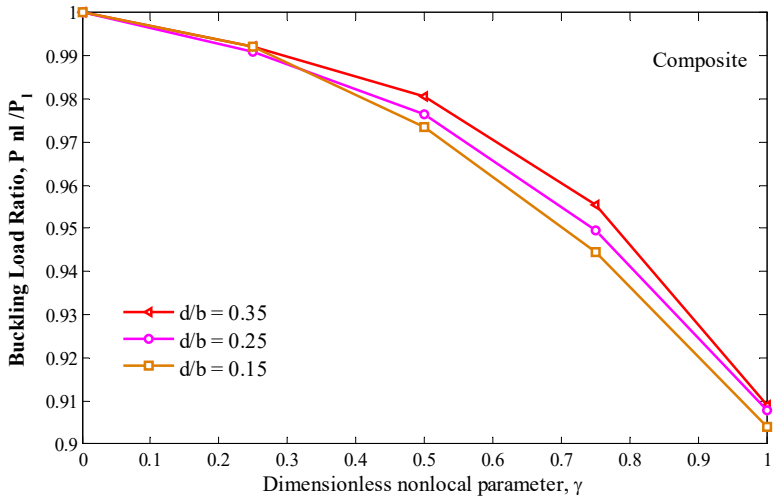

Fig. 6a

Fig. 6. Variation of the critical buckling load ratio by considering dimensionless nonlocal parameter for different length of square cut out in plate.

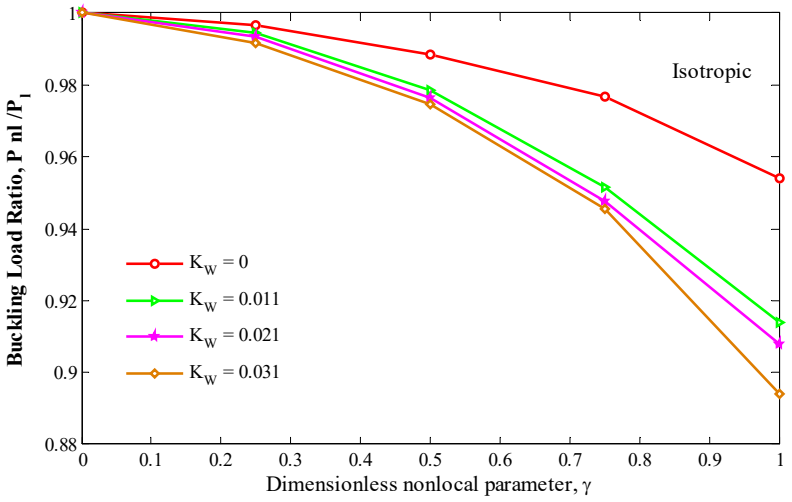

Fig. 7a

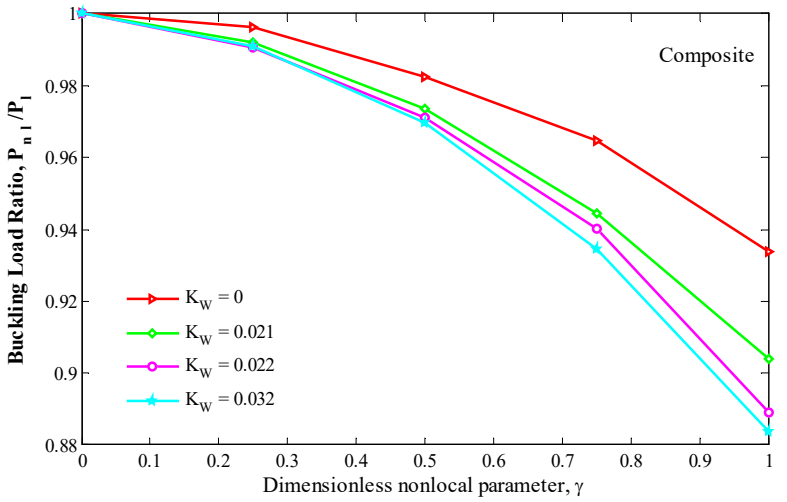

Fig. 7b

Fig. 7. Buckling load ratio versus dimensionless nonlocal parameter for different values of Winkler modulus parameter.

7. Conclusion

Buckling analysis of nano plate and nanocomposite plate with square cut out reinforced by CNTs subjected to uniaxial buckling load was investigated in this article. The plate was surrounded by Winkler foundation and Eringen's nonlocal elasticity theory was used to consider nanoscale effect. In order to define the shape function of cut out plate, domain decomposition method and orthogonal polynomials were applied. Finally, Rayleigh-Ritz energy method was used to obtain critical buckling load of system so that the impact of the dimensions of plate, length of square cut out and elastic medium on critical buckling load of nano plate and nanocomposite plate were distinguished. Results provided that by applying CNT as amplifier in plate increases the properties of system. In addition, by increasing dimensions of plate the buckling load ratio of plate with square cut out rises. Moreover, Existence a hole in plate causes defect in system and weaken the buckling behavior, therefore, by increasing length of square cut out in plate buckling load ratio increase. The other is that, considering Winkler modulus parameter improves the buckling behavior of plate.

References

[1] Murmu, T., and Pradhan, S. C., "Buckling of biaxially compressed orthotropic plates at small scales," Mechanics Research Communications, Vol. 36, pp. 933-938, 2009.

[2] Pradhan, S. C., "Buckling of single layer graphene sheet based on nonlocal elasticity and higher order shear deformation theory," Physics Letters A, Vol. 373, pp. 4182-4188, 2009.

[3] Aksencer, T., and Aydogdu, M., "Levy type solution method for vibration and buckling of nanoplates using nonlocal elasticity theory," Physica E: Low-dimensional Systems and Nanostructures, Vol. 43, pp. 954-959, 2011.

[4] Hashemi, S. H., and Samaei, A. T., "Buckling analysis of micro/nanoscale plates via nonlocal elasticity theory," Physica E: Low-dimensional Systems and Nanostructures, Vol. 43, pp. 1400-1404, 2011.

[5] Samaei, A. T., Abbasion, S., and Mirsayar, M. M., "Buckling analysis of a single-layer graphene sheet embedded in an elastic medium based on nonlocal Mindlin plate theory," Mechanics Research Communications, Vol. 38, pp. 481-485, 2011.

[6] Farajpour, A., Danesh, M., and M. Mohammadi, "Buckling analysis of variable thickness nanoplates using nonlocal continuum mechanics," Physica E: Low-dimensional Systems and Nanostructures, Vol. 44, pp. 719-727, 2011.

[7] Farajpour, A., Shahidi, A. R., Mohammadi, M., and Mahzoon, M., "Buckling of orthotropic micro/nanoscale plates under linearly varying in-plane load via nonlocal continuum mechanics," Composite Structures, Vol. 94, pp. 1605-1615, 2012.

[8] Murmu, T., Sienz, J., Adhikari, S., and Arnold, C., "Nonlocal buckling of double-nanoplate-systems under biaxial compression," Composites Part B: Engineering, Vol. 44, pp. 84-94, 2013.

[9] Radić, N., Jeremić, D., Trifković, S., and Milutinović, M., "Buckling analysis of double-orthotropic nanoplates embedded in Pasternak elastic medium using nonlocal elasticity theory," Composites Part B: Engineering, Vol. 61, pp. 162-171, 2014.

[10] Golmakani, M. E., and Rezatalab, J., "Nonuniform biaxial buckling of orthotropic nanoplates embedded in an elastic medium based on nonlocal Mindlin plate theory," Composite Structures, Vol. 119, pp. 238-250, 2015.

[11] Arani, A. G., Maghamikia, S., Mohammadimehr, M., and Arefmanesh, A., "Buckling analysis of laminated composite rectangular plates reinforced by SWCNTs using analytical and finite element methods," Journal of Mechanical Science and Technology, Vol. 25, pp. 809-820, 2011.

[12] Jam, J. E., and Maghamikia, S., "Elastic buckling of composite plate reinforced with carbon nano tubes," International Journal of Engineering Science and Technology, Vol. 3, pp. 4090-4101, 2011.

[13] Mohammadimehr, M., Mohandes, M., and Moradi, M., "Size dependent effect on the buckling and vibration analysis of double-bonded nanocomposite piezoelectric plate reinforced by boron nitride nanotube based on modified couple stress theory," Journal of Vibration and Control, 2014.

[14] Asadi, E., and Jam, J. E., "Analytical and Numerical Buckling Analysis of Carbon Nanotube Reinforced Annular Composite Plates," Int J Advanced Design and Manufacturing Technology, Vol. 7, pp. 35-44, 2014.

[15] Mohammadimehr, M., Rousta-Navi, B., and Ghorbanpour-Arani, A., "Biaxial Buckling and Bending of Smart Nanocomposite Plate Reinforced by CNTs using Extended Mixture Rule Approach," Mechanics of Advanced Composite Structures, Vol. 1, pp. 17-26, 2014.

[16] Ghorbanpour Arani, A., Jamali, M., Mosayyebi, M., and Kolahchi, R., "Wave propagation in FG-CNT-reinforced piezoelectric composite micro plates using viscoelastic quasi-3D sinusoidal shear deformation theory," Composites Part B: Engineering, Vol. 95, pp. 209-224, 2016.

[17] Ghorbanpour Arani, A., Jamali, M., Ghorbanpour-Arani, A., Kolahchi, R., and Mosayyebi, M., "Electro-magneto wave propagation analysis of viscoelastic sandwich nanoplates considering surface effects," Proceedings of the Institution of Mechanical Engineers, Part C: Journal of Mechanical Engineering Science, 2016.

[18] Wattanasakulpong, N., and Chaikittiratana, A., "Exact solutions for static and dynamic analyses of carbon nanotube-reinforced composite plates with Pasternak elastic foundation," Applied Mathematical Modelling, Vol. 39, pp. 5459-5472, 2015.
[19] Ashoori Movassagh, A., and Mahmoodi, M. J., "A micro-scale modeling of Kirchhoff plate based on modified strain-gradient elasticity theory," European Journal of Mechanics - A/Solids, Vol. 40, pp. 50-59, 2013.
[20] Ghorbanpour Arani, A., and Shokravi, M., "Vibration response of visco-elastically coupled double-layered visco-elastic graphene sheet systems subjected to magnetic field via strain gradient theory considering surface stress effects," Proceedings of the Institution of Mechanical Engineers, Part N: Journal of Nanoengineering and Nanosystems, 2014.
[21] Ghorbanpour Arani, A., Jamali, M., Mosayyebi, M., and Kolahchi, R., "Analytical modeling of wave propagation in viscoelastic functionally graded carbon nanotubes reinforced piezoelectric microplate under electro-magnetic field," Proceedings of the Institution of Mechanical Engineers, Part N: Journal of Nanoengineering and Nanosystems, 2015.
[22] Pan, Z., Cheng, Y., and Liu, J., "A semi-analytical analysis of the elastic buckling of cracked thin plates under axial compression using actual non-uniform stress distribution," Thin-Walled Structures, Vol. 73, pp. 229-241, 2013.
[23] Ghorbanpour Arani, A., Kolahchi, R., Mosayyebi, M., and Jamali, M., "Pulsating fluid induced dynamic instability of visco-double-walled carbon nano-tubes based on sinusoidal strain gradient theory using DQM and Bolotin method," International Journal of Mechanics and Materials in Design, pp. 1-22, 2014.
[24] Reddy, J. N., "Mechanics of Laminated Composite Plates and Shells: Theory and Analysis," second edition ed: CRC Press, 2003.
[25] Ghorbanpour Arani, A., Kolahchi, R., and Vossough, H., "Buckling analysis and smart control of SLGS using elastically coupled PVDF nanoplate based on the nonlocal Mindlin plate theory," Physica B: Condensed Matter, Vol. 407, pp. 4458-4465, 2012.
[26] Lam, K. Y., Hung, K. C., and Chow, S. T., "Vibration analysis of plates with cutouts by the modified Rayleigh-Ritz method," Applied Acoustics, Vol. 28, pp. 49-60, 1989.
[27] Lam K. Y., and Hung, K. C., "Orthogonal polynomials and sub-sectioning method for vibration of plates," Computers & Structures, Vol. 34, pp. 827-834, 1990.
[28] Liew, K. M., Hung, K. C., and Lim, M. K., "Method of domain decomposition in vibrations of mixed edge anisotropic plates," International Journal of Solids and Structures, Vol. 30, pp. 3281-3301, 1993.
[29] Liew, K. M., Hung, K. C., and Sum, Y. K., "Flexural vibration of polygonal plates: treatments of sharp re-entrant corners," Journal of Sound and Vibration, Vol. 183, pp. 221-238, 1995.
[30] Liew, K. M., Kitipornchai, S., Leung, A. Y. T., and Lim, C. W., "Analysis of the free vibration of rectangular plates with central cut-outs using the discrete Ritz method," International Journal of Mechanical Sciences, Vol. 45, pp. 941-959, 2003.
[31] Bhat, R. B., " Natural frequencies of rectangular plates using characteristic orthogonal polynomials in rayleigh-ritz method," Journal of Sound and Vibration, Vol. 102, pp. 493-499, 1985.
[32] Lam, K. Y., and Hung, K. C., "Vibration study on plates with stiffened openings using orthogonal polynomials and partitioning method," Computers & Structures, Vol. 37, pp. 295-301, 1990.
[33] Liew, K. M., Ng, T. Y., and Kitipornchai, S., "A semi-analytical solution for vibration of rectangular plates with abrupt thickness variation," International Journal of Solids and Structures, Vol. 38, pp. 4937-4954, 2001.
[34] Shams, S., and Soltani, B., "Buckling of Laminated Carbon Nanotube-Reinforced Composite Plates on Elastic Foundations Using a Meshfree Method," Arabian Journal for Science and Engineering, Vol. 41, pp. 1981-1993, 2016.
[35] Pradhan, S. C., and Murmu, T., "Small scale effect on the buckling of single-layered graphene sheets under biaxial compression via nonlocal continuum mechanics," Computational Materials Science, Vol. 47, pp. 268-274, 2009.